Molecular Ecology

WILEY

MOLECULAR ECOLOGY

ORIGINAL ARTICLE

Transcriptional Responses to Priority Effects in Nectar Yeast

Callie R. Chappell[1] | Pagé C. Goddard[2] | Lexi-Ann Golden[3] | Jonathan Hernandez[1] | Daniela Ortiz Chavez[4] | Marziiah Hossine[1,5] | Sur Herrera Paredes[6] | Ethan VanValkenburg[1] | Lucas A. Nell[1] | Tadashi Fukami[1,7] | Manpreet K. Dhami[1,8,9]

[1]Department of Biology, Stanford University, Stanford, California, USA | [2]Department of Genetics, Stanford University, Stanford, California, USA | [3]University of Michigan Medical School, Ann Arbor, Michigan, USA | [4]Department of Biochemistry and Molecular Genetics, University of Colorado Anschutz Medical Campus, Aurora, Colorado, USA | [5]Cellular and Molecular Biology, California State University, Northridge, Northridge, California, USA | [6]International Laboratory for Human Genome Research, Universidad Nacional Autónoma de México (UNAM), Juriquilla Querétaro, Querétaro, Mexico | [7]Department of Earth System Science, Stanford University, Stanford, California, USA | [8]Biocontrol and Molecular Ecology, Manaaki Whenua – Landcare Research, Lincoln, New Zealand | [9]School of Biological Sciences, University of Auckland, Auckland, New Zealand

Correspondence: Callie R. Chappell (calliech@stanford.edu) | Tadashi Fukami (fukamit@stanford.edu)

Received: 1 February 2024 | **Revised:** 20 September 2024 | **Accepted:** 30 September 2024

Handling Editor: Sarah Perry Flanagan

Tadashi Fukami and Manpreet K. Dhami are co-senior authors

Funding: This study was supported by the National Science Foundation (DEB 1149600, DEB 1737758), Community Science Program (CSP) grant from the Joint Genome Institute (https://doi.org/10.46936/10.25585/60001130), and Stanford University's Terman Fellowship. Part of this work was conducted by the U.S. Department of Energy Joint Genome Institute (https://ror.org/04xm1d337), a DOE Office of Science User Facility. The JGI is supported by the Office of Science of the U.S. Department of Energy operated under Contract No. DE-AC02-05CH11231. CRC was supported by a National Science Foundation Graduate Research Fellowship (DGE 1656518), a Stanford Graduate Fellowship, and a National Science Foundation Postdoctoral Research Fellowship in Biology (DBI 2305961). MKD was supported by Marsden Fund Grant (MFP-LCR-2002). SHP was supported by the Life Sciences Research Foundation. LG and JH were supported by the Stanford Department of Biology VPUE Biology Summer Research Program. DOC and MH were supported by the Stanford Summer Research Program. LAN was supported by the NSF Postdoctoral Fellowship in Biology (DBI 1401312).

Keywords: ecological genomics | eQTL | niche preemption | population genomics

ABSTRACT

Priority effects, where the order and timing of species arrival influence the assembly of ecological communities, have been observed in a variety of taxa and habitats. However, the genetic and molecular basis of priority effects remains unclear, hindering a better understanding of when priority effects will be strong. We sought to gain such an understanding for the nectar yeast *Metschnikowia reukaufii* commonly found in the nectar of our study plant, the hummingbird-pollinated *Diplacus* (*Mimulus*) *aurantiacus*. In this plant, *M. reukaufii* can experience strong priority effects when it reaches flowers after other nectar yeasts, such as *M. rancensis*. After inoculation into two contrasting types of synthetic nectar simulating early arrival of *M. rancensis*, we conducted whole-transcriptome sequencing of 108 strains of *M. reukaufii*. We found that several genes were differentially expressed in *M. reukaufii* strains when the nectar had been conditioned by growth of *M. rancensis*. Many of these genes were associated with amino acid metabolism, suggesting that *M. reukaufii* strains responded molecularly to the reduction in amino acid availability caused by *M. rancensis*. Furthermore, investigation of expression quantitative trait loci (eQTLs) revealed that genes involved in amino acid transport and resistance to antifungal compounds were enriched in some genetic variants of *M. reukaufii*. We also found that gene expression was associated with population growth rate, particularly when amino acids were limited. These results suggest that intraspecific genetic variation in the ability of nectar yeasts to respond to nutrient limitation and direct fungal competition underpins priority effects in this microbial system.

1 | Introduction

One particularly challenging type of interspecific interactions to predict are those that are historically contingent, where the outcome depends on the order and timing of species arrival (Drake, Huxel, and Hewitt 1996; Fukami 2010; Palmgren 1926). These interactions, called priority effects, can be a major source of unexplained variation in the species composition of ecological communities (Chase 2010; Delory et al. 2019; Song, Fukami, and Saavedra 2021). An increasing number of studies have sought to gain a better understanding of how and when priority effects operate because this understanding can allow some of the apparently random variation in species composition among local communities to be explained as a predictable outcome of history-dependent species interactions (Debray et al. 2022; Fukami 2015; Palmgren 1926; Stroud et al. 2024; Vellend 2010).

The ultimate cause of priority effects is positive feedback that makes initial conditions important to community assembly (De Meester et al. 2016; Ke and Letten 2018). Therefore, knowledge of the mechanisms of this positive feedback is key to explaining priority effects. Two groups of such mechanisms are niche preemption and niche modification (Fukami 2015). In niche preemption, early-arriving species deplete resources, limiting the growth of later-arriving species. In niche modification, early-arriving species change the local environment, for example, by releasing an inhibitory compound, altering the growth of a later-arriving species. However, how species respond to niche preemption or niche modification remain poorly described in many systems. Understanding how species differ in their response to niche preemption and niche modification helps to predict when priority effects will be strong (Grainger et al. 2019).

Niche modification and preemption can vary not just among species, but also among genetically variable populations within species (Urban and De Meester 2009). Such intraspecific variation makes priority effects even more difficult to understand, but this variation at the same time provides a largely unexploited opportunity to study how genetic variation influences individuals' molecular response to priority effects. By connecting population-level genetic variation with differences in transcriptional responses, we can better understand how genetic variation influences how priority effects play out. However, few studies have made this connection.

In this paper, we report an experimental study where we used transcriptomics to identify genes that might be responsible for niche preemption and modification in a microbial system (Figure 1A). Previously, we sequenced and annotated the whole genome of the nectar-inhabiting yeast *Metschnikowia reukaufii*, which suggested that their resistance to priority effects against a closely related species *Mestchnikowia rancensis* might be due to extensive duplications of nitrogen transport genes (Dhami, Hartwig, and Fukami 2016). To explore the role of intraspecific genetic variation on this species, we had also conducted whole genome resequencing of 108 *M. reukaufii* strains isolated from the hummingbird-pollinated shrub *Diplacus* (formerly *Mimulus*) *aurantiacus* (Dhami et al. 2018). In this study, we found that the 108 strains grouped into three distinct lineages that were associated with metabolic ability and resistance to priority effects. Here, we build on these previous studies to conduct RNA sequencing on the 108 strains of *M. reukaufii* in two experimentally created nectar conditions, one mimicking priority effects by a competitor, to better understand the genetic basis of within-species differences in the strength of priority effects. For this purpose, we investigated whether the strains varied in the patterns of gene expression. We also examined whether the strains express genes differently depending on the nectar environment they grow in, which would represent an instance of phenotypic plasticity (de Nadal, Ammerer, and Posas 2011; Rivera et al. 2021).

2 | Materials and Methods

2.1 | Microbial Growth and Sampling

A total of 108 isolates of *M. reukaufii* reported in Dhami et al. (2018) (Figure 1B,C and Table S1) were plated from glycerol stocks that had been kept at −80°C on yeast mould (YM) agar and incubated at 25°C for 2 days. Previously, each of the 108 isolates of *M. reukaufii* had been sequenced, genotyped, and clustered into genetically distinct groups using FastSTRUCTURE (k = 4), which is reproduced in Figure 1C (Dhami et al. 2018). An additional rooted ML tree was built using Treemix (1.13) by grouping SNPs to account for linkage disequilibrium (k = 1000) and accounting for migration (Figure S2 and Data S3). A single isolated colony on each of these plates was inoculated into YM broth and shaken at 200 rpm for 2 days at 25°C. Cells were pelleted at 3000 rpm for 5 min and washed twice with sterile phosphate buffered saline (PBS). After measuring optical density at 600 nm (OD_{600}), cells were inoculated at a final density of 2×10^2 cells/μL into 3 mL of synthetic nectar into the two nectar treatments, either the high amino acid nectar or *M. rancensis*-conditioned nectar. Four replicates per treatment were shaken at 200 rpm for 10 h at 25°C and harvested by pelleting at 3724 g for 5 min at 25°C. The pellet was flash frozen in liquid nitrogen for subsequent RNA extraction. All 864 samples were grown and processed in a single batch over a single 48 h period. Samples were stored at −80°C until further use.

We prepared synthetic nectar to mimic *D. aurantiacus* nectar in amino acid and sugar composition (Peay, Belisle, and Fukami 2012). Specifically, the synthetic nectar contained fructose (4%), glucose (2%), sucrose (20%), serine (0.102 mM), glycine (0.097 mM), proline (0.038 mM), glutamate (0.035 mM), aspartic acid (0.026 mM), GABA1 (0.023 mM), and alanine (0.021 mM). All components were mixed in water until dissolved, filtered through a 0.2 μm filter, and stored at −20°C until used. The first treatment increased the amino acid concentration in nectar to 10× the concentration of the standard nectar, to mimic a rich environment. The second treatment was prepared exactly the same as the first treatment, except that it was conditioned by *Metschnikowia rancensis*, which is closely related to *M. reukaufii* (Peay, Belisle, and Fukami 2012; Pozo et al. 2016) and has previously been shown to engage in strong priority effects with *M. reukaufii* (Dhami, Hartwig, and Fukami 2016; Dhami et al. 2018; Grainger et al. 2019; Peay, Belisle, and Fukami 2012; Vannette and Fukami 2014).

Adding multiple species to the same nectar would have been a more conventional approach to evaluate the effect of

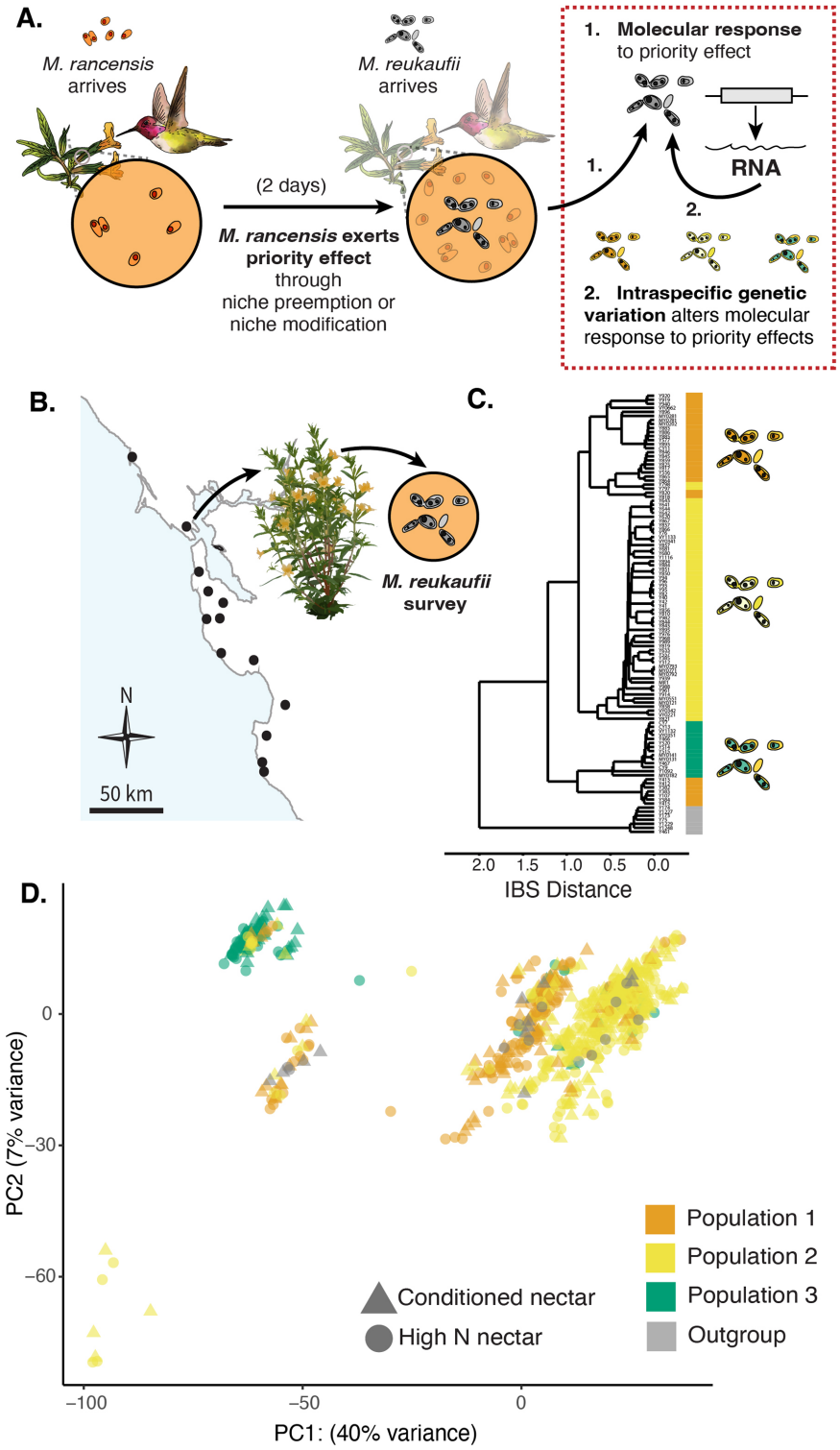

FIGURE 1 | Sub-populations of nectar yeast differ in transcriptional response. (A) Schematic of this study where early-arriving *Metschnikowia rancensis* exerts a priority effect on *M. reukaufii* in the nectar of *D. aurantiacus* through niche preemption or niche modification. We report (1) the molecular response of *M. reukaufii* to priority effects exerted by *M. rancensis* and (2) the effect of intraspecific genetic variation within *M. reukaufii* on its molecular response to priority effects by *M. rancensis*. (B) Wild yeast were isolated from the nectar of *Diplacus aurantiacus* growing at 12 sites in and around the San Francisco Bay Area of California, USA. (C) Whole genome resequencing of 108 strains of nectar yeast *Metschnikowia reukaufii* revealed three populations (Dhami et al. 2018). (D) In the current study, 108 strains of *M. reukaufii* were grown separately in synthetic *D. aurantiacus* nectar with high amino acid or synthetic nectar conditioned with competitor yeast *M. rancensis*. After 10 h of growth, overall gene expression was predominantly influenced by population group (colour) and less by nectar treatment (shape) (PERMANOVA, population group: $N = 742$, $R^2 = 0.028$, $p = 0.009$). *M. reukaufii* grown in high amino acid nectar are circles versus conditioned nectar as triangles. There was no significant difference between nectar treatments (PERMANOVA, nectar treatment: $N = 718$, $R^2 = 0.0007$, $p = 0.60$). Each point represents an individual replicate. Outgroup strains are Y1227, Y1229, Y1248, Y173, and Y142.

interspecific interactions. However, because our focal species *M. reukaufii* and competitor *M. rancensis* are closely related, it would have been challenging to identify whether RNA reads came from *M. reukaufii* or *M. rancensis*. To avoid this problem, we used nectar where *M. rancensis* was grown, but then filtered out. This conditioned nectar treatment represents a similar environment to what *M. reukaufii* may encounter if *M. rancensis* arrives early to a flower and draws down amino acids in nectar before *M. reukaufii* arrives, while eliminating the need to disentangle RNA reads from two closely related species in co-culture. *M. rancensis*-conditioned nectar was prepared by growing *M. rancensis* in the normal synthetic nectar for 48 h at 25°C and shaking at 200 rpm. *M. rancensis* was removed from the nectar by centrifugation at 6000 g for 5 min, followed by filtration of supernatant through a 0.02 μm filter. To ensure that yeast cells and RNA had been sufficiently removed in the final conditioned nectar, we used a MOBIO PowerWater RNA Isolation Kit (MO BIO Laboratories, Carlsbad, CA) to extract residual RNA. Less than 9 ng/μL of RNA was detected in the conditioned nectar.

2.2 | RNA Extraction, Library Preparation, and Sequencing

RNA was extracted from 864 cell pellets using a phenol-chloroform extraction method (Collart and Oliviero 1993; Eggermont, Goderis, and Broekaert 1996). Pellets were resuspended in phenol, chloroform, and isoamyl alcohol with an RNA extraction buffer, and incubated at 60°C for 30 min while shaking. RNA was extracted using phase separation and centrifugation with phenol, chloroform, and isoamyl alcohol. RNA was precipitated using a lithium chloride solution and incubated at −20°C overnight. Samples were centrifuged, and the pellet resuspended in cold 80% ethanol. After pelleting again, the ethanol was removed and the purified RNA was resuspended in pyrogen-free water and stored at −80°C. Diluted RNA was treated with DNase I using a Zymo DNase I kit (Zymo Research, Irvine, CA) and purified using a Zymo RNA Clean and Concentrator Kit (Zymo Research, Irvine, CA). Final RNA concentrations were quantified using an Invitrogen Quant-iT Broad Range RNA Assay Kit (Thermo Fisher, Waltham, MA). Purified RNA was shipped to the Joint Genome Institute (JGI), where cDNA libraries were generated using an TruSeq RNA Library Prep Kit (Illumina, San Diego, CA). Samples were sequenced on a NovaSeq 6000 sequencer (2 × 251 bp reads). JGI provided cleaned, trimmed reads for bioinformatic analysis. BBDuk (version 38.25) was used to remove contaminants, trim reads of adapter sequences, and remove reads with low quality scores. BBMap (Bushnell 2014) was used to map reads to an *M. reukaufii* reference genome (Dhami, Hartwig, and Fukami 2016) and reads that mapped to human, cat, dog, or mouse references at 93% identity were filtered, along with ribosomal sequences. Reads were pre–processed using BBDuk (JGI 2021) for quality trimming and filtering, then aligned to the reference genome (Dhami, Hartwig, and Fukami 2016) using HISAT2 (2.2.0) (Kim, Langmead, and Salzberg 2015). deepTools (v3.1) (Ramírez et al. 2014) was used to generate strand-specific bigWig files and raw gene counts were generated using featureCounts (Liao, Smyth, and Shi 2014).

2.3 | Differential Expression Analysis

In R (3.5.2), DESeq2 (Love et al. 2014) was used to generate a differential expression count matrix, using a raw read count matrix as the input. After an inverse normalisation transformation, the transformed count matrix was used in principal component analysis (PCA) and differences between groups were analysed by PERMANOVA with Bray–Curtis Dissimilarity using the `adonis` function in vegan (2.5-7) (Oksanen et al. 2019). After log normalisation, independent hypothesis weighting was used to determine the number of significantly differentially expressed genes per treatment ($p < 0.1$, FDR = 0.1). Significantly differentially expressed genes ($p < 0.05$, LFC < 0.5 or > 0.5) are reported in Table S4. We predicted the function of expressed genes using the InterPro database (`interproscan` *5.45–80.0*) (Blum et al. 2021). TopGO (2.46.0) was used to identify enriched GO terms in significantly differentially expressed genes (Alexa and Rahnenführer 2009). GO term enrichment was examined for Biological Process (BP) (Figure 2B), Cellular Component (CC), and Molecular Function (MF) based on the "weight01" algorithm and Fisher statistic (Figure S5 and Table S5).

2.4 | cis-eQTL Mapping and Functional Annotation

Pre- and post-processing of the cis-eQTL data were performed in R (4.0.3). Strains with no genotype data, and samples with fewer than 4,000,000 RNA-seq library reads were excluded from eQTL calling. In the RNA-seq dataset, samples corresponding to the Y76 strain had exceptionally low read counts relative to the rest of the dataset (mean = 1,557,935 vs. 10,582,904 reads). A minimum library size of four million reads provided an arbitrary cutoff that cleanly separated these low-expression samples from the rest.

Only genes with at least 0.1 TPM (transcript per kilobase million) and five or more read counts in at least 144 samples (20% of samples) were retained for analysis. Genes on scaffolds without complete genotype information were excluded from cis-eQTL mapping. Raw gene count estimates were converted to counts per million (cpm) using the `cpm` function from edgeR (Robinson, McCarthy, and Smyth 2010), then inverse-normalised using the `RankNorm` function from RNOmni (McCaw et al. 2020). Principal components (PCs) were calculated from the transformed count data using PCATools (Blighe, 2018/2022), and the number of PCs to include in the final model was determined using the Gavish-Donoho method (Gavish and Donoho 2014).

eQTL mapping was performed using tensorQTL in Python (3.9.8) (Taylor-Weiner et al. 2019). Eight samples representing the Y76 strain were excluded from analysis due to low library size, an additional 32 samples representing the Y413, Y962, and Y983 strains were excluded due to a lack of genotype data, and 77 samples across 44 strains were removed from analysis due to lack of RNA-seq data, leaving 718 remaining samples across both conditions for eQTL calling. Lack of genotype information for scaffolds 117 and 100 led to the exclusion of 1398 and 2 genes, respectively. Of the remaining 4589 annotated genes, 252 genes

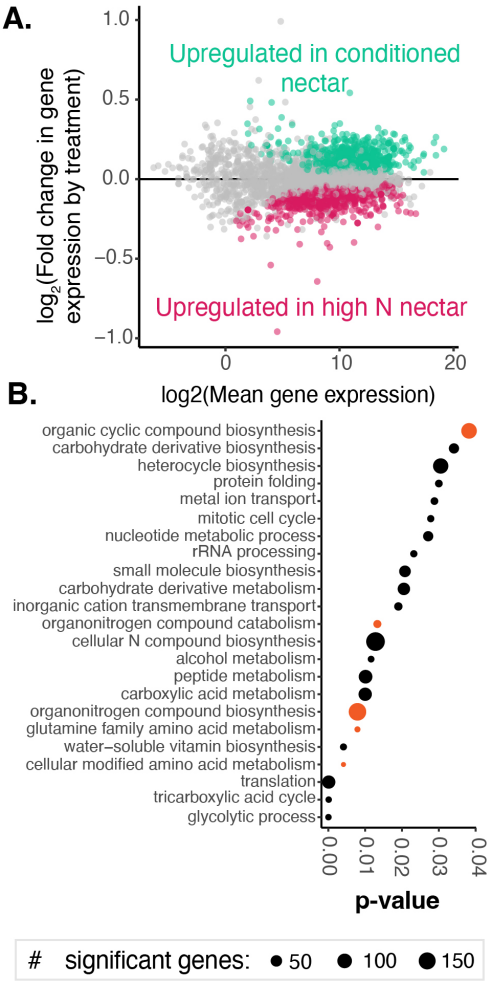

FIGURE 2 | Transcriptional differences based on nectar treatment. (A) Significantly differentially expressed genes ($n = 6613$) between treatments, high amino acid nectar (bottom, magenta) and *M. rancensis*-conditioned nectar (top, teal). Each point represents an individual gene. (B) Enriched biological process gene ontology (GO) terms in significantly differentially expressed genes ($n = 2520$). The size of each bubble denotes the number of significant genes with that GO term. GO terms coloured in orange are associated with amino acid metabolism or catabolism.

were removed from analysis due to low expression, resulting in 4337 (94.5%) genes for eQTL analysis. No variants were dropped. Variants within 1 Mb of the transcription start site were tested for association with gene expression and genotype using a linear model with an interaction term. The model included sample strain, group, collection site, sequencing plate, and the first 33 PCs as covariates:

$$\text{expression} \sim \text{genotype} + \text{nectar condition} + \text{genotype} \times \text{nectar condition} + \text{strain} + \text{group} + \text{collection site} + \text{sequencing plate} + \text{PCs}$$

In this model, expression represents the level of RNA for a particular gene present in the sample. Genotype does not refer to the strain of *M. reukaufii*. Rather, we use the term genotype to refer to the individual genetic polymorphism (variant) present at a particular site in the genome, such as A versus T. For example, at a single site at the genome (e.g., the 764027th base pair on scaffold (chromosome) 4), a SNP can either be C/C (homozygous for the reference allele C), C/A (heterozygous), or A/A (homozygous for the alternate allele A), depending on the strain. There are two alleles since this yeast has a diploid genome. The nectar condition is whether the sample was grown in conditioned or high amino acid nectar. The strain represents which sequenced *M. reukaufii* isolate was grown, in which genetically distinct group (Group 1, 2, or 3 in Figure 1). The collection site (where the yeast was originally collected from), sequencing plate, and principal components (PCs) representing the aggregated additional experimental variation were also included in the model. The top eQTL variant was reported for each gene, and corrected for multiple testing by multiplying the nominal p-values to the effective number of tests reported by *tensorQTL*'s eigenMT option. Response eQTL genes were defined by a significant interaction term (Bonferroni-corrected, adjusted p-value ≤ 0.05).

We predicted the function of expressed genes using the InterPro database (`interproscan` 5.45–80.0) [4]. TopGO (2.46.0) was used to identify enriched GO terms in genes associated with interaction. GO term enrichment was examined for Biological Process (BP) based on the "weight01" algorithm and Fisher statistic.

2.5 | Metabolomics Analysis

The nectar (supernatant) from a subset of samples ($n = 192$) presented above were analysed for targeted amino acid quantification (Table S6). Supernatant nectar was stored at −80°C. After thawing, 700 µL of the sample was filtered through 0.22-µm Costar Spin-X cellulose acetate filter tubes (Corning Inc., Corning, NY) for 5 min (13,000 rpm, 20°C). Samples were then lyophilised and resuspended in 1 mL methanol containing a 1× internal standard. Internal standards were ^{13}C-labelled amino acids, summarised in Table S7, as well as labelled inosine, trehalose, mannitol and adenine. Calibration curves were generated using seven high and conditioned control nectars at the following concentrations of each internal standard: (1) 10×, (2) 5×, (3) 1×, (4) 0.5×, (5) 0.1×, (6) 0.05×, (7) 0.01×. An extraction control with empty tubes was also conducted. All samples and controls were vortexed for 3–5 s, sonicated for 10 min, and centrifuged for 5 min (5000 rpm, 4°C). The supernatant was then transferred to 0.22-µM Costar Spin-X cellulose acetate filter tubes (Corning Inc., Corning, NY) and centrifuged for 2.5 min (2500 rpm, 4°C). Filtrate was transferred to LCMS vials for polar (HILIC) LC–MS. Samples were run using UHPLC normal phase chromatography on an Agilent 1290 LC stack and a Q Exactive HF Orbitrap MS (Thermo Scientific). MS and HILIC methods are described in detail here (Domeignoz-Horta et al. 2023). Using average peak area in negative ionisation mode, we created a standard curve for each amino acid to calculate the concentration within each sample. Amino acids where the concentration was less than or equal to that detected in the negative controls were removed from the analysis. To calculate the amount of each amino acid secreted or consumed in the nectar, and the concentration of each amino acid in each sample was subtracted from the average concentration in the negative controls. A t-test was used to compare changes in each

amino acid concentration between nectar treatments and population groupings (groups 1, 2, and 3).

2.6 | Growth Phenotyping

To assay yeast growth in nectar with varying amino acid concentrations, we used two synthetic nectars similar to that described in Section 2.1. One was low amino acid nectar, using the same relative concentrations of amino acids as in the standard nectar used in the main experiment reported in Section 2.1, but reducing the overall concentration of amino acids by 1/10×. The other was high amino acid nectar, with a 2× concentration of amino acids. Because the two experiments (i.e., those described in Sections 2.1 and 2.6) did not use an identical pair of nectar environments, we cannot make direct comparisons between the two, but as detailed in the results section, the experiments nonetheless yielded broadly consistent results, both indicating that gene expressions depended strongly on amino acid availability.

To assay growth, we first streaked 12 strains of *M. reukaufii* (Y382, Y383, Y385, Y466, Y467, Y644, Y818, Y821, Y858, Y893, Y1092, MR1) from a glycerol stock onto a yeast malt agar (YMA) plate. These strains were phylogenetically dispersed across the three populations and had varying morphologies. We incubated plates of each strain at 26°C for 2–3 days. For each repetition of each treatment for each strain, we homogenised a single plated colony into yeast malt (YM) broth to create an overnight culture that was incubated at 26°C while shaking at 200 rpm for 16 h. Next, we rinsed the overnight cultures to separate them from the nutrient-dense YM broth. We vortexed each culture, centrifuged 200 μL solution at 6000 *g* for 5 min on an Eppendorf 5415D (Eppendorf, Germany), decanted the liquid using a pipette, and then added 200 μL normal amino acid synthetic nectar. We repeated this process for a second rinse and resuspended in nectar of the appropriate type for each treatment. Rinsed cultures were then diluted to 10^{-4} using the treatment's nectar type. We incubated 10 μL of these rinsed, diluted cultures at 26°C and used the remainder for plating to estimate the starting colony forming unit (CFU) counts. After one day, we plated the incubated cultures for final CFU counts. For starting CFU counts, we plated using additional 10^{0}, 10^{-1}, 10^{-2}, and 10^{-3} dilutions using sterile 0.85% NaCl solution; for final CFU counts, we used 10^{-1}, 10^{-2}, and 10^{-3} dilutions. For all CFU counts, we used spot plating onto YMA plates with 10 μL per spot and 3 technical replicates. Plates were counted after 48 h of incubation at 26°C. To estimate growth rates, we conducted a linear regression for each strain of per-capita growth (log[final CFU/starting CFU]) on starting density (starting CFU). The y-intercepts from these regressions can be regarded as the predicted maximum population growth rates since they are the estimated growth rates when the starting densities approach zero.

The relationship between the estimated maximum growth rate in either low or high amino acid nectar and the level of gene transcription for the corresponding strain was then assessed. Growth rates were averaged across replicates and regressed against average Fragments Per Kilobase of transcript per Million mapped reads (FPKM) across replicates using a Spearman's rank correlation test. In this analysis, we examined the top 110 most differentially expressed genes, which had an adjusted *p*-value of < 0.00001. For each gene, those strains in which no gene expression was detected were excluded from the analysis. In examining the expression-growth relationships, final *p*-values were adjusted using a Bonferroni correction to take into account the multiple tests that were conducted to investigate 110 genes.

We used a general independence test (`coin` V3) to determine whether there were more genes that were associated with growth (−log10(*p*-value)) in the high versus low amino acid nectar treatments and if so, whether the absolute value of that association (to account for differences in directionality) was significantly different between high and low amino acid nectar treatments.

3 | Results

3.1 | Transcriptome Sequencing and Alignment

A total of 12,559,122,137 raw reads were obtained from all samples. After quality control, an average of 14,428,231 (85%) of clean reads per sample mapped to the *M. reukaufii* MR1 reference genome (Dhami, Hartwig, and Fukami 2016) (Tables S1 and S2, Figure S1). Distributions of mapped reads were similar between the two nectar-type treatments.

3.2 | Population-Level Response to the Nectar Environment

Previously, the 108 strains of *M. reukaufii* used here were isolated from wild *D. aurantiacus* flowers, sequenced and genotyped using GATK (Dhami et al. 2018). From these 108 strains, three distinct population genotypes of *M. reukaufii* were identified using the model-based Bayesian algorithm fastSTRUCTURE and an identity-by-state (IBS) phylogenetic tree with a non-*M. reukaufii Metschnikowia* sp. outgroup ($n = 7$) (Dhami et al. 2018; Raj, Stephens, and Pritchard 2014, Figure 1C). We refer to the groups described in Dhami et al. (2018) as populations in this paper, following the convention in population genomics. Thus, by populations, we do not necessarily mean spatially defined entities. Here, we found that samples that were from similar populations were more likely to have more similar gene expression overall (Figure 1D) (PERMANOVA, population group: $n = 718$, $R^2 = 0.028$, $p = 0.009$). In fact, they clustered according to our three, previously identified populations (Figure 1C). In addition, we found two clusters that consisted of strains belonging to population 1 (Figure 1D), which corresponded to the two genetically distinct subgroups of population 1 (Figure 1C). Population 1 appeared to be polyphyletic due to gene flow and admixture between populations 1 and 2 (Figure S2 and Table S3). There was no statistically significant difference between the nectar treatments (PERMANOVA, nectar treatment: $n = 718$, $R^2 = 0.0007$, $p = 0.60$).

3.3 | Functional Enrichment of Differentially Expressed Genes

Although there was no overall significant difference in transcription, on a per sample basis, by treatment, individual genes

did differ in expression by treatment. A total of 4972 genes had a nonzero total read count when mapped to the reference *M. reukaufii* MR1 genome (Dhami et al. 2018) (Figures S3 and S4). Of these, 1177 (20%) genes were more highly expressed in the high amino acid nectar, and 886 (15%) were more highly expressed in the conditioned nectar after accounting for independent hypothesis weighting ($p_{adj.} < 0.1$, nominal FDR control = 0.1) (Figure 2A and Table S4). Of differentially expressed genes, 1657 (90%) had predicted functions. Biological processes enriched in differentially expressed genes by treatment included cellular nitrogen biosynthesis ($n = 193$, $p = 0.01$) and organonitrogen compound biosynthesis ($n = 165$, $p = 0.08$) (Figure 2B, Table S5 and Figure S5).

3.4 | eQTLs

Previously, single nucleotide polymorphisms (SNPs) and inserts and deletions (InDels) were called for the strains using GATK (Dhami et al. 2018; McKenna et al. 2010). Variants were filtered using GATK (version 3.4) and VCFtools (version1.5) (Danecek et al. 2011). eQTL mapping was performed using these 88,193 SNPs and 4111 genes, testing the association between genotype and transcriptional response to the two nectar treatments. Here, we use the definition of genotype used in population genomics, which refers to how variation at a specific site in the genome (e.g., a single A or T) is associated with differences in expression of a single RNA transcript. Thus, our test for the association between genotype and transcriptional response is a comparison between a single portion of the genome (a single DNA site) with a unique RNA transcript. We tested whether this association between genotype and transcriptional response differed between environments (nectar treatment) or had an interacting effect between the genotype and environment (interaction effect) (Figure S6 and Table S6). We observed 355 genes whose expression was associated with genotype (genotype eQTLs), and 176 with treatment-dependent genotype associations (interaction eQTLs, Figure 3A). Only 39 genes were shared between genotype and interaction eQTLs. The effect sizes of significant eQTLs were similar between treatment, genotype, and the interaction between them (Figure 3B). Generally, treatment, genotype, and interaction eQTLs had the same direction of effect (Figure S5).

The top GO terms of genes associated with interaction eQTLs included ion transport pathways (Figure 3C). For example, a predicted aminotransferase involved in the N starvation response (Figure 4A) (adj. $p_{GxE} = 0.013$) and an ATP-binding cassette (ABC) transporter was differentially affected by genotype and nectar treatment (adj. $p_{GxE} = 0.002$) (Figure 4B) (Table S6).

3.5 | Metabolomics

We identified three amino acids where the degree to which they were secreted or consumed differed significantly between high and conditioned nectar (Figure 5). The degree to which phenylalanine was secreted or consumed also differed based on the population from which each yeast strain came (Figure 5A).

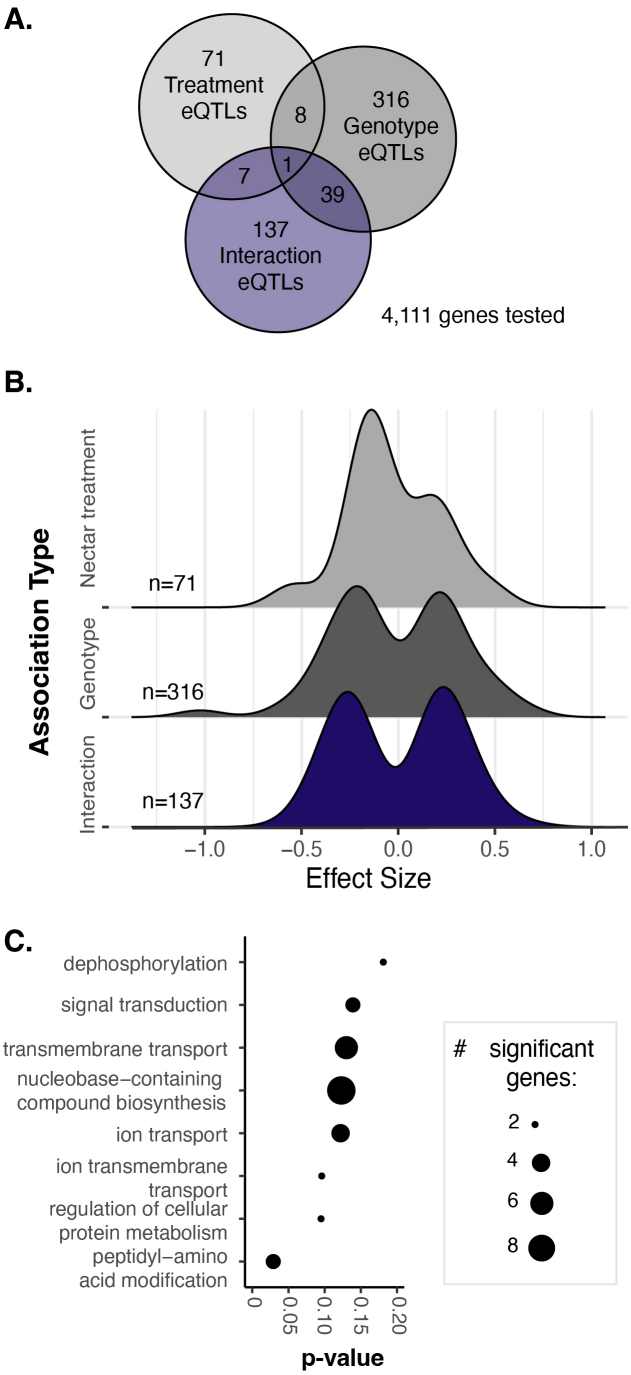

FIGURE 3 | Expression QTLs by treatment, genotype, and interaction. (A) Summary of eQTLs by treatment, genotype, and the interaction between them. (B) Frequency distribution of effect sizes of eQTLs by treatment, genotype, and interaction. (C) GO term enrichment of interaction eQTLs.

3.6 | Growth Phenotyping

Across the top 110 most differentially expressed genes, the adjusted *p*-values for the relationship between gene expression and growth rate across the 12 strains examined were significantly smaller in the low amino acid nectar treatment than in the high amino acid nectar ($Z = -2.53$, $p = 0.01$; Figure 6A). Of the 110 genes, 13 genes showed a significant association between the level of expression and the estimated maximum growth rate

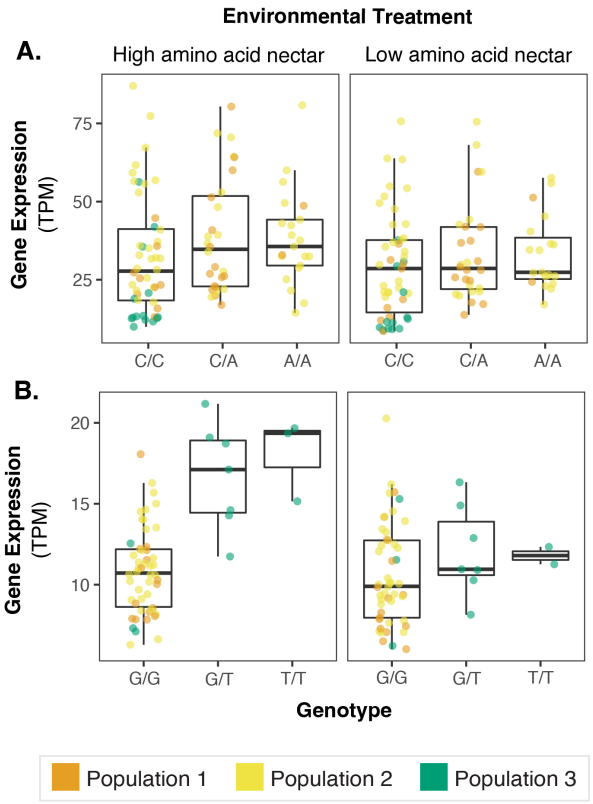

FIGURE 4 | Differential expression by genotype and treatment. Differential expression of two specific genes by genotype. Here, genotype refers to variation of a single nucleotide (A, T, C, or G) at a single site in the genome. Two nucleotides are presented at each site since the *M. reukaufii* genome is diploid and a single nucleotide polymorphism (SNP) can be homozygous or heterozygous for either the reference or alternative allele at each SNP. These are presented as examples to demonstrate patterns that may be found across other genes and sites. (A) Expression (transcript per kilobase million, or TPM) of a putative amino acid transporter (transcript 38,411) differs based on genotype at SNP 764027 and nectar treatment (adj. $p_{GxE}=0.013$, effect size $=0.100\pm0.022$), suggesting a gene-by-environment interaction. (B) Expression (TPM) of a putative ABC transporter (transcript 35,539) based on genotype at SNP 1047038 and nectar treatment (adj. $p_{GxE}=0.002$, effect size $=-0.370\pm0.075$). Individual points represent gene expression within an individual sample (e.g., the expression level of transcript 35,539 in a strain with C/C at SNP 764027), including technical replicates ($n=4$) per strain. Points are coloured by whether the sample (strain) was from population 1, 2, or 3 (Figure 1C).

in either low or high amino acid nectar (Table S8). Only three genes of these 13 had a significant association in the high amino acid nectar, whereas all of the remaining 10 showed a significant trend only in the low amino acid nectar. For example, we found that strains that were slower to grow relative to other strains had a higher level of transcription of a predicted histidine phosphatase (transcript 117,768) in low amino acid nectar, $r(11)=-0.80$, $p_{adj}=1.7\times10^{-7}$; Figure 6B, but no such relationship was found in high amino acid nectar, $r(9)=-0.24$, $p_{adj}=0.45$; Figure 6C. Moreover, across the top 110 genes, the association between growth and gene expression was significantly stronger when the strains grew in low amino acid nectar than in high amino acid nectar ($Z=2.04$, p-value $=0.04$; Figure S7).

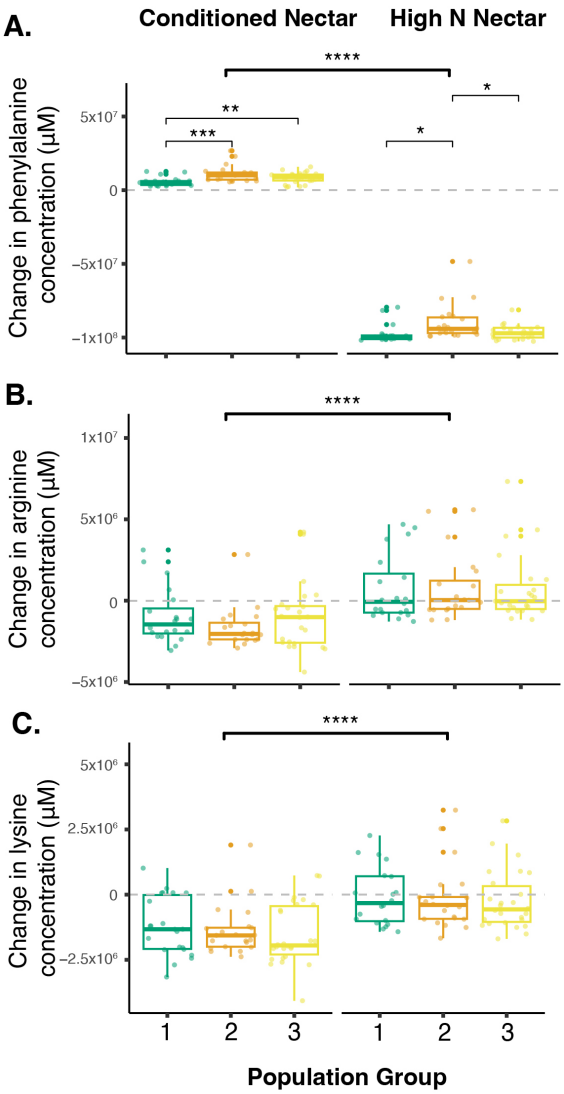

FIGURE 5 | Amino acid consumption or excretion by nectar treatment and population group. Change in the concentration of phenylalanine, arginine, and lysine relative to control nectar differed between conditioned and high amino acid nectar treatments. Each point represents an individual sample (strain), where we measured amino acid concentration, with four biological replicates per strain. (A) Change in phenylalanine concentration (μM), when compared to control nectar, by nectar type and population group. Some population groups differed in their phenylalanine consumption or excretion. (B) Change in arginine concentration (μM), when compared to control nectar, by nectar type and population group. (C) Change in lysine concentration (μM), when compared to control nectar, by nectar type and population group.

4 | Discussion

We found that early arrival of *M. rancensis* altered gene expressions in *M. reukaufii* differently depending on *M. reukaufii* strain identity. In particular, functional analysis of genes that were differentially expressed between the two nectar environments found enrichment associated with cellular nitrogen biosynthesis and organonitrogen compound biosynthesis (Figure 2B). In nectar, competition for amino acids

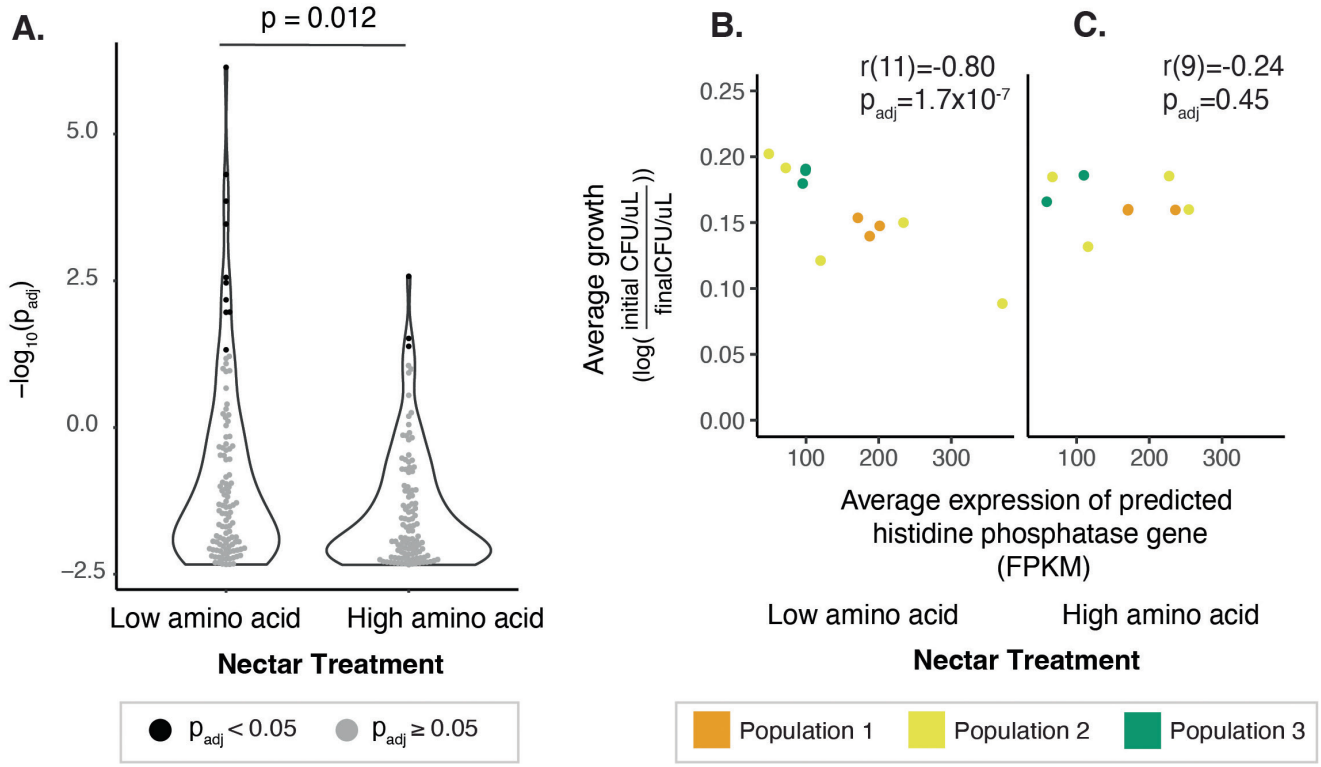

FIGURE 6 | Association between growth and transcription of a predicted histidine phosphatase gene. (A) Across the top 110 most differentially expressed genes, more genes were significantly associated with growth in the low amino acid nectar treatment than in the high amino acid nectar treatment ($Z = -2.53$, $p = 0.01$). Each point represents a gene. (B and C) Spearman rank correlation between yeast growth of 12 *M. reukaufii* strains and expression of a predicted histidine phosphatase gene (transcript 117,768) in either low amino acid nectar $r(11) = -0.80$, $p_{adj} = 1.7 \times 10^{-7}$or high amino acid nectar, $r(9) = -0.24$, $p_{adj} = 0.45$. Each point represents a sample (strain) where growth was measured in our experiment. We highlight this predicted histidine phosphatase gene as an example of a gene where differential expression was associated with differences in yeast growth.

between *M. reukaufii* and other yeast species such as *M. rancensis* can be severe (Dhami et al. 2018; Grainger et al. 2019; Letten et al. 2018; Peay, Belisle, and Fukami 2012; Vannette and Fukami 2014). When *M. rancensis* arrives first to a *D. aurantiacus* flower via a hummingbird, *M. rancensis* can rapidly deplete amino acids in nectar. Thus, to resist priority effects by *M. rancensis*, a late-arriving *M. reukaufii* strain would have to express genes that help them survive in low nitrogen environments. Indeed, our differential expression analysis showed that *M. reukaufii* changes expression of genes associated with competition for amino acids due to the early arrival of *M. rancensis*. This finding is broadly consistent with our prior genome analysis of *M. reukaufii*, which revealed extensive gene duplications in high-capacity amino acid transporters (Dhami, Hartwig, and Fukami 2016). We speculate that the limited nitrogen availability in the form of amino acids, an essential N resource for microbial growth, have exerted strong selection pressure in the evolution of *M. reukaufii* (Dhami et al. 2018).

A surprising finding from this study is how strongly genotypic identity influences the yeasts' transcriptional response to early arrival of *M. rancensis*. Prior work identified three groups within this collection of *M. reukaufii* strains (Dhami et al. 2018) (Figure 1C). Our results suggest that the three groups do not always respond in the same way to priority effects. By combining population-level genetic variation (Figure 1) and differences in gene expression (Figure 2), we identified several genes whose expression level differed based on yeast lineage (*cis* eQTLs) (Figure 3).

Two examples of eQTLs illustrate how our results suggest lineage-specific mechanisms of priority effects. First, variation at SNP 764027 demonstrates how the interaction between genotype and the environment can strongly alter expression of a putative amino acid transporter (transcript 38,411) (Figure 4A). This gene, which is predicted to help import amino acids into the cell, was more highly expressed when *M. rancensis* had depleted amino acids. Increased expression of a putative amino acid import gene in nectar environment conditioned by a competitor suggests niche preemption as a mechanism of priority effects. This hypothesis is supported by the previous studies showing that *Metschnikowia* yeast species drew down amino acid concentration in nectar (Peay, Belisle, and Fukami 2012; Vannette and Fukami 2014, 2018), that competition for amino acids in nectar altered competitive outcomes (Tucker and Fukami 2014; Grainger et al. 2019), and that gene expression levels of select N scavenging genes increased in microcosm competition experiments (Dhami, Hartwig, and Fukami 2016). We found that in the conditioned nectar treatment, earlyarriving *M. rancensis* drew down nectar N, making the late-arriving *M. reukaufii* express amino acid transporters to scavenge for the remaining amino acids. Our results build on prior findings, suggesting that the extent to which *M. reukaufii* can scavenge for N also depends on the genotype: heterozygous strains at

SNP 764027 are able to express that gene more highly than those with either homozygous strains.

In a second example, there was increased expression of a transcript (35539) depending on the genotype at SNP 1047038 and depending on nectar treatment. However, the effect of genotype was greatly reduced in the high amino acid nectar environment (Figure 4B). This gene is predicted to be an ABC transporter, which can support resistance to antifungal compounds (Kumari et al. 2021). In the nectar conditioned by *M. rancensis*, potentially containing antifungal compounds that inhibit *M. reukaufii* growth (Álvarez-Pérez et al. 2016), M. reukaufii's expression of this ABC transporter differed based on its genotype at SNP 1047038. This second example suggests niche modification as a mechanism of priority effects, where *M. rancensis* could prevent the growth of later-arriving *M. reukaufii* by producing a toxic compound (Álvarez-Pérez et al. 2016). Prior work has shown how *M. reukaufii* and other nectar microbes can be affected by secondary metabolites (Mueller, Francis, and Vannette 2023; Vannette and Fukami 2018), with secondary effects on pollinator foraging (Vannette and Fukami 2016). Production of toxic compounds or chemicals that alter microbial behaviour such as quorum sensing could affect community dynamics in nectar (Álvarez-Pérez, Lievens, and Fukami 2019).

Here, we show that the interactive effect of environment (such as niche preemption by *M. rancensis*) and genotype can alter how species respond to competition. Thus, the effects of intraspecific genetic variation within *M. reukaufii* can only be understood in their environmental context. The two examples discussed, as well as the 137 additional interaction eQTLs (Figure 3A), suggest that neither yeast genotype nor nectar environment alone fully explains the transcriptional response to priority effects. Instead, the interplay between genotype and environment is necessary to understand how species interact.

Differences in the expression of some genes between treatments were associated with differential growth rate among strains in both high and low amino acid nectars. However, this link between gene expression and growth rate was more apparent when strains were grown in low amino acid nectar than in high amino acid nectar (Figure 6). Although the nectar treatments were different between the two experiments, preventing us from making direct comparisons, the results nonetheless suggest that gene expression depends on amino acid availability. Further, these findings suggest that differences in gene expression among the strains matter more for population growth in nectar when *M. reukaufii* strains grow under low amino acid conditions, as they would if another competitive yeast species like *M. rancensis* established in nectar before *M. reukaufii* arrives, than when they grow under high amino acid conditions, which would be the case if *M. reukaufii* arrived before *M. rancensis*. In other words, strain-specific gene expression influences growth more strongly when amino acids are depleted by early-arriving competitors, suggesting that these genes may underlie priority effects in the nectar yeast studied here.

Additionally, we have shown how intraspecific variation within *M. reukaufii* may alter its interaction with the environment. By measuring targeted amino acids in nectar before and after yeast growth, we found that some amino acid abundance was altered in environment-specific (nectar type) and gene-specific (population) manners (Figure 5). These differences may explain how priority effects arise through niche preemption and modification in this system. For example, theory predicts that priority effects occur if species deplete the resources that are more essential to other species than to themselves more greatly than they deplete the resources more essential to themselves (Chase and Leibold 2003; Tilman 1980). Because *M. reukaufii* and *M. rancensis* differ in their consumption and growth limitation with respect to different amino acids that are available in nectar (Vannette and Fukami 2014), this prediction may apply to the nectar yeasts. In this study, however, we did not attempt to determine whether the assumptions of any specific theoretical model are met in the nectar yeast system. The data presented in this paper do not identify an exact cause or mechanism of priority effects. The data, however, lay a foundation for future identification of the genes responsible for niche preemption or modification in nectar yeast species.

In summary, we have sought to connect population-level genetic variation to differences in molecular traits (gene expression) associated with priority effects. Although it is difficult to tease apart exact mechanisms of priority effects, here we used our results to speculate on the molecular basis of niche preemption and modification as mechanisms of priority effects. To more directly test for the effects of the proposed genes, future research would benefit from generating transgenic *M. reukaufii* with knock-out genes or eQTLs identified in this study.

Author Contributions

C.R.C., M.K.D., and T.F. designed and conducted the research. E.V.V. and L.A.N. conducted the growth phenotyping. C.R.C., P.C.G., L.-A.G., J.H., D.O.C., M.H., and S.H.P. analysed the data. C.R.C. and T.F. wrote the paper, and all authors contributed to improving the paper.

Acknowledgements

We thank Laura Bogar, Ben Bowen, Glade Dlott, Hunter Fraser, Adina Howe, Grant Kinsler, Katherine Louie, Trent Northen, Lauren O'Connell, Kabir Peay, Dmitri Petrov, Gavin Sherlock, Nasa Sinnott-Armstrong, Rachel Vannette, Tuya Yokoyama, four anonymous reviewers, and the members of the community ecology group at Stanford for discussion and comments. We also thank Ben Bowen, Katherine Louie, Trent Northen, Christa Pennacchio, and other staff at JGI for assistance with metabolomics. This work was supported by the National Science Foundation (DEB 1149600, DEB 1737758), Community Science Program (CSP) grant from the Joint Genome Institute (https://doi.org/10.46936/10.25585/60001130), and Stanford University's Terman Fellowship. Part of this work was conducted by the U.S. Department of Energy Joint Genome Institute (https://ror.org/04xm1d337), a DOE Office of Science User Facility. The JGI is supported by the Office of Science of the U.S. Department of Energy operated under Contract No. DE-AC02-05CH11231. CRC was supported by a National Science Foundation Graduate Research Fellowship (DGE 1656518), a Stanford Graduate Fellowship, and a National Science Foundation Postdoctoral Research Fellowship in Biology (DBI 2305961). MKD was supported by Marsden Fund Grant (MFP-LCR-2002). SHP was supported by the Life Sciences Research Foundation. LG and JH were supported by the Stanford Department of Biology VPUE Biology Summer Research Program. DOC and MH were supported by the Stanford Summer Research Program. LAN was supported by the NSF Postdoctoral Fellowship in Biology.

Conflicts of Interest

The authors declare no conflicts of interest.

Data Availability Statement

Genetic Data: Raw sequence reads are downloadable from the JGI Genome Portal (FD 1202157; SP 1202175; AP 1202158). Individual genotype data, sample metadata, and analyses are available on GitLab: https://gitlab.com/teamnectarmicrobe/n01_nectar_yeast_transcriptomics. Sample Metadata: Metadata are also stored on GitLab: https://gitlab.com/teamnectarmicrobe/n01_nectar_yeast_transcriptomics. Benefits generated: This research occurred in collaboration with several undergraduate researchers, whose training in ecology, evolution, and genomics was advanced through this work. Broadly, our group is committed to advancing diversity, equity, and inclusion in the life sciences.

References

Alexa, A., and J. Rahnenführer. 2009. "Gene Set Enrichment Analysis With topGO." *Bioconductor Improv* 27: 1–26.

Álvarez-Pérez, S., C. de Vega, M. I. Pozo, et al. 2016. "Nectar Yeasts of the Metschnikowia Clade Are Highly Susceptible to Azole Antifungals Widely Used in Medicine and Agriculture." *FEMS Yeast Research* 16, no. 1: fov115. https://doi.org/10.1093/femsyr/fov115.

Álvarez-Pérez, S., B. Lievens, and T. Fukami. 2019. "Yeast–Bacterium Interactions: The Next Frontier in Nectar Research." *Trends in Plant Science* 24, no. 5: 393–401. https://doi.org/10.1016/j.tplants.2019.01.012.

Blighe, K. 2022. "*PCAtools: Everything Principal Component Analysis* [R Package Version 2.10.0]." https://github.com/kevinblighe/PCAtools (Original work published 2018).

Blum, M., H.-Y. Chang, S. Chuguransky, et al. 2021. "The InterPro Protein Families and Domains Database: 20 Years on." *Nucleic Acids Research* 49, no. D1: D344–D354. https://doi.org/10.1093/nar/gkaa977.

Bushnell, B. 2014. "*BBMap: A Fast, Accurate, Splice-Aware Aligner*." https://www.semanticscholar.org/paper/BBMap%3A-A-Fast%2C-Accurate%2C-Splice-Aware-Aligner-Bushnell/f64dd54444a724574deb7710888091350eebb2b9.

Chase, J. M. 2010. "Stochastic Community Assembly Causes Higher Biodiversity in More Productive Environments." *Science* 328, no. 5984: 1388–1391. https://doi.org/10.1126/science.1187820.

Chase, J. M., and M. A. Leibold. 2003. *Ecological Niches*. University of Chicago Press. https://www.press.uchicago.edu/ucp/books/book/chicago/E/bo3638660.html.

Collart, M. A., and S. Oliviero. 1993. "Preparation of Yeast RNA." *Current Protocols in Molecular Biology* 13, no. 12: 1–13.12.5.

Danecek, P., A. Auton, G. Abecasis, et al. 2011. "The Variant Call Format and VCFtools." *Bioinformatics* 27, no. 15: 2156–2158. https://doi.org/10.1093/bioinformatics/btr330.

De Meester, L., J. Vanoverbeke, L. J. Kilsdonk, and M. C. Urban. 2016. "Evolving Perspectives on Monopolization and Priority Effects." *Trends in Ecology & Evolution* 31, no. 2: 136–146. https://doi.org/10.1016/j.tree.2015.12.009.

de Nadal, E., G. Ammerer, and F. Posas. 2011. "Controlling Gene Expression in Response to Stress." *Nature Reviews Genetics* 12, no. 12: 833–845. https://doi.org/10.1038/nrg3055.

Debray, R., R. A. Herbert, A. L. Jaffe, A. Crits-Christoph, and B. Koskella. 2022. "Priority Effects in Microbiome Assembly." *Nature Reviews Microbiology* 20, no. 2: 109–121. https://doi.org/10.1038/s41579-021-00604-w.

Delory, B. M., E. W. A. Weidlich, P. von Gillhaussen, and V. M. Temperton. 2019. "When History Matters: The Overlooked Role of Priority Effects in Grassland Overyielding." *Functional Ecology* 33, no. 12: 2369–2380. https://doi.org/10.1111/1365-2435.13455.

Dhami, M. K., T. Hartwig, and T. Fukami. 2016. "Genetic Basis of Priority Effects: Insights From Nectar Yeast." *Proceedings of the Royal Society of London B: Biological Sciences* 283, no. 1840: 20161455. https://doi.org/10.1098/rspb.2016.1455.

Dhami, M. K., T. Hartwig, A. D. Letten, M. Banf, and T. Fukami. 2018. "Genomic Diversity of a Nectar Yeast Clusters Into Metabolically, But Not Geographically, Distinct Lineages." *Molecular Ecology* 27, no. 8: 2067–2076. https://doi.org/10.1111/mec.14535.

Domeignoz-Horta, L. A., G. Pold, H. Erb, et al. 2023. "Substrate Availability and Not Thermal Acclimation Controls Microbial Temperature Sensitivity Response to Long-Term Warming." *Global Change Biology* 29, no. 6: 1574–1590. https://doi.org/10.1111/gcb.16544.

Drake, J. A., G. R. Huxel, and C. L. Hewitt. 1996. "Microcosms as Models for Generating and Testing Community Theory." *Ecology* 77, no. 3: 670–677. https://doi.org/10.2307/2265489.

Eggermont, K., I. J. Goderis, and W. F. Broekaert. 1996. "High-Throughput RNA Extraction From Plant Samples Based on Homogenisation by Reciprocal Shaking in the Presence of a Mixture of Sand and Glass Beads." *Plant Molecular Biology Reporter* 14, no. 3: 273–279.

Fukami, T. 2010. "Community Assembly Dynamics in Space." *Community Ecology: Processes, Models, and Applications*, 45–54. http://web.stanford.edu/~fukamit/fukami-2010.pdf.

Fukami, T. 2015. "Historical Contingency in Community Assembly: Integrating Niches, Species Pools, and Priority Effects." *Annual Review of Ecology, Evolution, and Systematics* 46, no. 1: 1–23. https://doi.org/10.1146/annurev-ecolsys-110411-160340.

Gavish, M., and D. L. Donoho. 2014. "The Optimal Hard Threshold for Singular Values Is $4/\sqrt{3}$." *IEEE Transactions on Information Theory* 60, no. 8: 5040–5053. https://doi.org/10.1109/TIT.2014.2323359.

Grainger, T. N., A. D. Letten, B. Gilbert, and T. Fukami. 2019. "Applying Modern Coexistence Theory to Priority Effects." *Proceedings of the National Academy of Sciences* 116, no. 13: 6205–6210. https://doi.org/10.1073/pnas.1803122116.

JGI. 2021. "*BBDuk* [Computer Software]." https://sourceforge.net/projects/bbmap/.

Ke, P.-J., and A. D. Letten. 2018. "Coexistence Theory and the Frequency-Dependence of Priority Effects." *Nature Ecology & Evolution* 2, no. 11: 1691–1695. https://doi.org/10.1038/s41559-018-0679-z.

Kim, D., B. Langmead, and S. L. Salzberg. 2015. "HISAT: A Fast Spliced Aligner With Low Memory Requirements." *Nature Methods* 12, no. 4: 357–360. https://doi.org/10.1038/nmeth.3317.

Kumari, S., M. Kumar, N. A. Gaur, and R. Prasad. 2021. "Multiple Roles of ABC Transporters in Yeast." *Fungal Genetics and Biology* 150: 103550. https://doi.org/10.1016/j.fgb.2021.103550.

Letten, A. D., M. K. Dhami, P.-J. Ke, and T. Fukami. 2018. "Species Coexistence Through Simultaneous Fluctuation-Dependent Mechanisms." *Proceedings of the National Academy of Sciences* 115, no. 26: 6745–6750. https://doi.org/10.1073/pnas.1801846115.

Liao, Y., G. K. Smyth, and W. Shi. 2014. "featureCounts: An Efficient General Purpose Program for Assigning Sequence Reads to Genomic Features." *Bioinformatics* 30, no. 7: 923–930. https://doi.org/10.1093/bioinformatics/btt656.

Love, M. I., W. Huber, and S. Anders. 2014. "Moderated Estimation of Fold Change and Dispersion for RNA-Seq Data with DESeq2." *Genome Biology* 15, no. 12: 550. https://doi.org/10.1186/s13059-014-0550-8.

McCaw, Z. R., J. M. Lane, R. Saxena, S. Redline, and X. Lin. 2020. "Operating Characteristics of the Rank-Based Inverse Normal Transformation for Quantitative Trait Analysis in Genome-Wide Association Studies." *Biometrics* 76, no. 4: 1262–1272. https://doi.org/10.1111/biom.13214.

McKenna, A., M. Hanna, E. Banks, et al. 2010. "The Genome Analysis Toolkit: A MapReduce Framework for Analyzing Next-Generation

DNA Sequencing Data." *Genome Research* 20, no. 9: 1297–1303. https://doi.org/10.1101/gr.107524.110.

Mueller, T. G., J. S. Francis, and R. L. Vannette. 2023. "Nectar Compounds Impact Bacterial and Fungal Growth and Shift Community Dynamics in a Nectar Analog." *Environmental Microbiology Reports* 15, no. 3: 170–180. https://doi.org/10.1111/1758-2229.13139.

Oksanen, J., F. G. Blanchet, M. Friendly, et al. 2019. "*Vegan: Community Ecology Package* (Version 2.5-5) [Computer Software]." https://CRAN.R-project.org/package=vegan.

Palmgren, A. 1926. "Chance as an Element in Plant Geography." In *Proceedings of the International Congress of Plant Sciences*, edited by B. M. Duggar, 1, 591–602. Ithaca, NY.

Peay, K. G., M. Belisle, and T. Fukami. 2012. "Phylogenetic Relatedness Predicts Priority Effects in Nectar Yeast Communities." *Proceedings of the Royal Society of London B: Biological Sciences* 279, no. 1729: 749–758. https://doi.org/10.1098/rspb.2011.1230.

Pozo, M. I., C. M. Herrera, M.-A. Lachance, K. Verstrepen, B. Lievens, and H. Jacquemyn. 2016. "Species Coexistence in Simple Microbial Communities: Unravelling the Phenotypic Landscape of Co-Occurring *Metschnikowia* Species in Floral Nectar." *Environmental Microbiology* 18, no. 6: 1850–1862. https://doi.org/10.1111/1462-2920.13037/full.

Raj, A., M. Stephens, and J. K. Pritchard. 2014. "fastSTRUCTURE: Variational Inference of Population Structure in Large SNP Data Sets." *Genetics* 197, no. 2: 573–589. https://doi.org/10.1534/genetics.114.164350.

Ramírez, F., F. Dündar, S. Diehl, B. A. Grüning, and T. Manke. 2014. "deepTools: A Flexible Platform for Exploring Deep-Sequencing Data." *Nucleic Acids Research* 42, no. Web Server issue: W187–W191. https://doi.org/10.1093/nar/gku365.

Rivera, H. E., H. E. Aichelman, J. E. Fifer, et al. 2021. "A Framework for Understanding Gene Expression Plasticity and Its Influence on Stress Tolerance." *Molecular Ecology* 30, no. 6: 1381–1397. https://doi.org/10.1111/mec.15820.

Robinson, M. D., D. J. McCarthy, and G. K. Smyth. 2010. "edgeR: A Bioconductor Package for Differential Expression Analysis of Digital Gene Expression Data." *Bioinformatics* 26, no. 1: 139–140. https://doi.org/10.1093/bioinformatics/btp616.

Song, C., T. Fukami, and S. Saavedra. 2021. "Untangling the Complexity of Priority Effects in Multispecies Communities." *Ecology Letters* 24, no. 11: 2301–2313. https://doi.org/10.1111/ele.13870.

Stroud, J. T., B. M. Delory, E. M. Barnes, et al. 2024. "Priority Effects Transcend Scales and Disciplines in Biology." *Trends in Ecology & Evolution* 39, no. 7: 677–688. https://doi.org/10.1016/j.tree.2024.02.004.

Taylor-Weiner, A., F. Aguet, N. J. Haradhvala, et al. 2019. "Scaling Computational Genomics to Millions of Individuals With GPUs." *Genome Biology* 20, no. 1: 228. https://doi.org/10.1186/s13059-019-1836-7.

Tilman, D. 1980. "Resources: A Graphical-Mechanistic Approach to Competition and Predation." *American Naturalist* 116, no. 3: 362–393. https://doi.org/10.1086/283633.

Tucker, C. M., and T. Fukami. 2014. "Environmental Variability Counteracts Priority Effects to Facilitate Species Coexistence: Evidence From Nectar Microbes." *Proceedings of the Royal Society of London B: Biological Sciences* 281, no. 1778: 20132637. https://doi.org/10.1098/rspb.2013.2637.

Urban, M. C., and L. De Meester. 2009. "Community Monopolization: Local Adaptation Enhances Priority Effects in an Evolving Metacommunity." *Proceedings of the Royal Society of London B: Biological Sciences* 276, no. 1676: 4129–4138. https://doi.org/10.1098/rspb.2009.1382.

Vannette, R. L., and T. Fukami. 2014. "Historical Contingency in Species Interactions: Towards Niche-Based Predictions." *Ecology Letters* 17, no. 1: 115–124. https://doi.org/10.1111/ele.12204.

Vannette, R. L., and T. Fukami. 2016. "Nectar Microbes Can Reduce Secondary Metabolites in Nectar and Alter Effects on Nectar Consumption by Pollinators." *Ecology* 97, no. 6: 1410–1419. https://doi.org/10.1890/15-0858.1.

Vannette, R. L., and T. Fukami. 2018. "Contrasting Effects of Yeasts and Bacteria on Floral Nectar Traits." *Annals of Botany* 121, no. 7: 1343–1349. https://doi.org/10.1093/aob/mcy032.

Vellend, M. 2010. "Conceptual Synthesis in Community Ecology." *Quarterly Review of Biology* 85, no. 2: 183–206. https://doi.org/10.1086/652373.

Supporting Information

Additional supporting information can be found online in the Supporting Information section.